CrossMark

ORIGINAL RESEARCH

Double Differential Alpha, Proton and Deuteron Emission Cross Section Calculations for the Structural Fusion Materials ^{46,48}Ti

İsmail Hakki Sarpün

Abstract Double differential light charged particle emission cross section is a fundamental value to determine nuclear heating and material damages in structural fusion material development. In this study, double differential alpha, proton and deuteron emission cross sections for ^{46}Ti and ^{48}Ti target nuclei have been calculated by the TALYS 1.6 code at 15 MeV incident neutron energy. The light charged particles are emitted due to mainly three different processes—compound, direct and pre-equilibrium. The compound nucleus formation process dominates the emission of light charged particle up to 8 MeV emission energy. Pre-equilibrium and direct reaction contribution become dominant in higher particle emission energies. The calculated double differential cross sections have been compared with the available experimental data taken from the literature.

Keywords Light charged particle emission · Double differential cross section · Pre-equilibrium, compound and direct reactions · TALYS code

Introduction

Fusion reactors need proper structural materials to become an efficient source of energy, especially if the promise of a green machine is to be maintained. Reactor components, such as first wall, divertor, limiters and breeding blanket, are subjected not only to the high energy neutron impact, but also to strong mechanical, heat and electromagnetic loadings. These conditions compose a very severe operation framework for the structural materials and have led to a detailed research and development process for the candidate materials. The main idea in the candidate materials development is the development of low activation materials for the safety conditions [1].

While the fission process produces long lived actinides, the fusion reaction does not basically yield other radioactive elements. But neutrons due to deuterium (D)–tritium (T) fusion reaction will activate the reactor materials surrounding the plasma and this affects the waste management and disposal scenarios conditions. Under undesired conditions, the nuclear heating is an important parameter, since heat increase oxidation and possible volatilization and such release to the environment is the main contamination hazard in a loss of coolant condition [2]. In order to evaluate these parameters, extended cross section data libraries together with decay and activation data have been developed and according to the The European Activation System (EASY) [3], fusion reactor neutron spectra (first wall, blanket, shield and two magnetic coils) have been used to show that only a few primary elements (C, Si, Ti, Fe, Cr and V) can be considered. Other elements, such as W can be used in limited quantities. Moreover, all of the evaluations made up to present show the importance of the presence of typical tramp impurities present in these metals, such as Al, Ni, Ag, Co, Nb and others, that are detrimental because of their poor radiological properties [1].

Titanium and its alloys are an attractive structural material candidates for fusion reactors due to their favorable properties, such as high strength-to-weight ratio, intermediate strength values, good fatigue and creep rupture properties, small modulus of elasticity, high electrical resistivity, heat capacity, low coefficient of thermal expansion, low long-term (<10 years after shutdown)

İ. H. Sarpün (✉)
Physics Department, Afyon Kocatepe University,
Afyonkarahisar, Turkey
e-mail: isarpun@gmail.com

residual radioactivity (after V and Cr, Ti has the fastest decay rate), a high corrosion resistance together with good compatibility with coolants such as lithium, helium and water, high workability and good weldability and commercial availability with established mine and mill capacity [4]. Leguey et al. [5] have reported results after irradiation with 590 MeV energetic protons (mean dose rate is 3×10^{-6} dpa s^{-1} and mean He production rate is 50 appm/dpa) of pure Ti, for irradiation doses ranging between 10^{-3} and 10^{-1} dpa. Proton-irradiation at 330 K induces a significant increase in the critical stress measured at 0.2 % plastic strain and a decrease in the work hardening rate. Hardening is of the order of about 40 % per dpa for a dose of 0.03 dpa.

The biggest disadvantage of titanium and its alloys used as a fusion reactor material is their high chemical affinity with hydrogen which leads to hydrogen embrittlement and an expected large tritium inventory. Craighead et al. [6] reported that for impact embrittlement, a critical level of hydrogen concentration was required and that the onset of embrittlement was probably associated with precipitation of the hydride phase. Subsequently, Berger et al. [7], showed that additions of aluminum raise the critical level of hydrogen for embrittlement and this was tentatively attributed to an increase in the solubility limit. The hydrogen solubility in titanium was first estimated by Lenning et al. [8], to be less than 100 wppm below 523 K. The three major sources of hydrogen isotopes in a fusion reactor environment are: hydrogen produced in the metal by neutron transmutation reactions, interactions with the D–T fuel in the plasma chamber and interactions with tritium in the breeding material [4].

In a fusion reactor neutrons carry most of the energy produced by the D–T fusion reaction. Those neutrons lose their energy by interacting with reactor devices such as the blanket through various nuclear reactions and the heat produced by these nuclear reactions is called "nuclear heating" and is estimated by a simulation calculation in a reactor design. One of the essential data for simulation calculation is the energy and angular distributions of charged particles emitted by a nuclear reaction. These distributions are called "double differential cross section (DDX) data". Charged particle emission nuclear reactions from fusion device materials are complex due to contributions from sequential decays and multi-body break-up [9]. It is also quite important for estimating various physical quantities, such as primary knock-on atom (PKA) spectra, gas production per atom (GPA) and displacement per atom (DPA) [10]. Furthermore, the study of DDX is important as a basic study because the contributions of the direct and the pre-equilibrium processes as well as that of statistical compound nucleus process, in the emission of

light charged particles can be estimated for a given neutron induced reaction [11].

The DDX of light charged particle emission reactions have been investigated both experimentally [9, 11–17] and theoretically [18–23].

In this study, the theoretical DDX of alpha, proton and deuteron emission reactions for ^{46}Ti and ^{48}Ti target nuclei, fusion structural materials, at the incident neutron energy of 15 MeV have been calculated. The results have been also compared with the experimental data in literature.

Calculation Methods

In this study, DDX calculations were performed using the pre-equilibrium exciton model and the Hauser–Feshbach model implemented in the TALYS 1.6 code. The pre-compound model implements new expressions for internal transition rates and new parameterization of the average squared matrix element for the residual interaction obtained using the optical model potential from Ref. [24].

The TALYS code was developed to analyze and predict nuclear reactions involving neutrons, photons and light charged particles ($A \leq 4$) in the energy range of 1 keV– 1 GeV for target nuclei heavier than lithium [25]. The default model of the pre-equilibrium process in TALYS is the two-component exciton model (EM) where the time evolution of the nuclear state is described by the total energy of the system and the total number of nucleons above the Fermi surface and corresponding holes below it. A detailed description of the model is available in Ref. [26]. TALYS includes the phenomenological model proposed by Kalbach [27] to take into account the nucleon transfer (NT) and the knock-out (KO) reactions which are not included in the exciton model. The total pre-equilibrium (PE) cross section is sum of these three contributions:

$$\frac{d\sigma^{PE}}{dE} = \frac{d\sigma^{EM}}{dE} + \frac{d\sigma^{NT}}{dE} + \frac{d\sigma^{KO}}{dE}$$

Results and Conclusions

The double differential cross section ($d^2\sigma/d\Omega \cdot dE$) for the emission of proton, deuteron and alpha particles at emission angles 45°, 60°, 75° and 135° for incident neutron energy 15.0 MeV have been calculated using TALYS 1.6 for ^{46}Ti and ^{48}Ti target nuclei. The calculated energy distribution of the emitted light charged particles has been compared with available experimental data of Grimes et al. [28] taken form the EXFOR [29] nuclear data library.

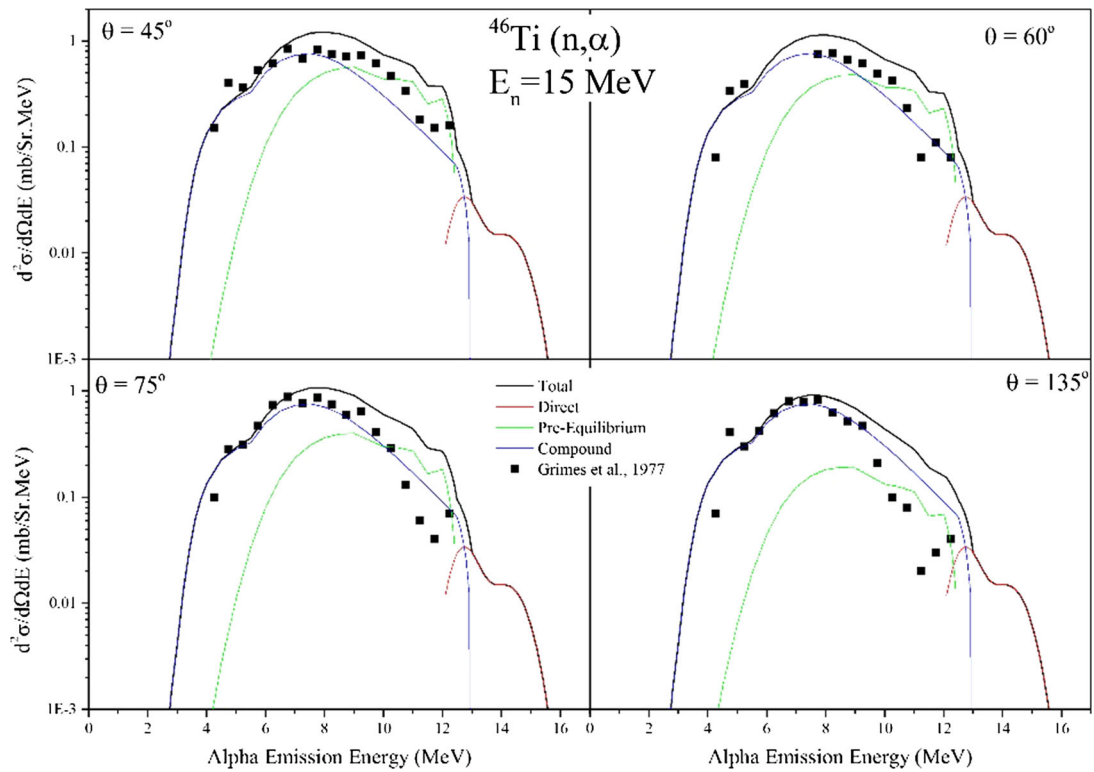It can be seen from the Figs. 1, 2, 3, 4, 5, and 6 that theoretically calculated DDX results using TALYS 1.6

Fig. 1 The comparison of calculated DDX of (n,α) reaction on ^{46}Ti with the experimental data reported in literature. Experimental values were taken from EXFOR [29]
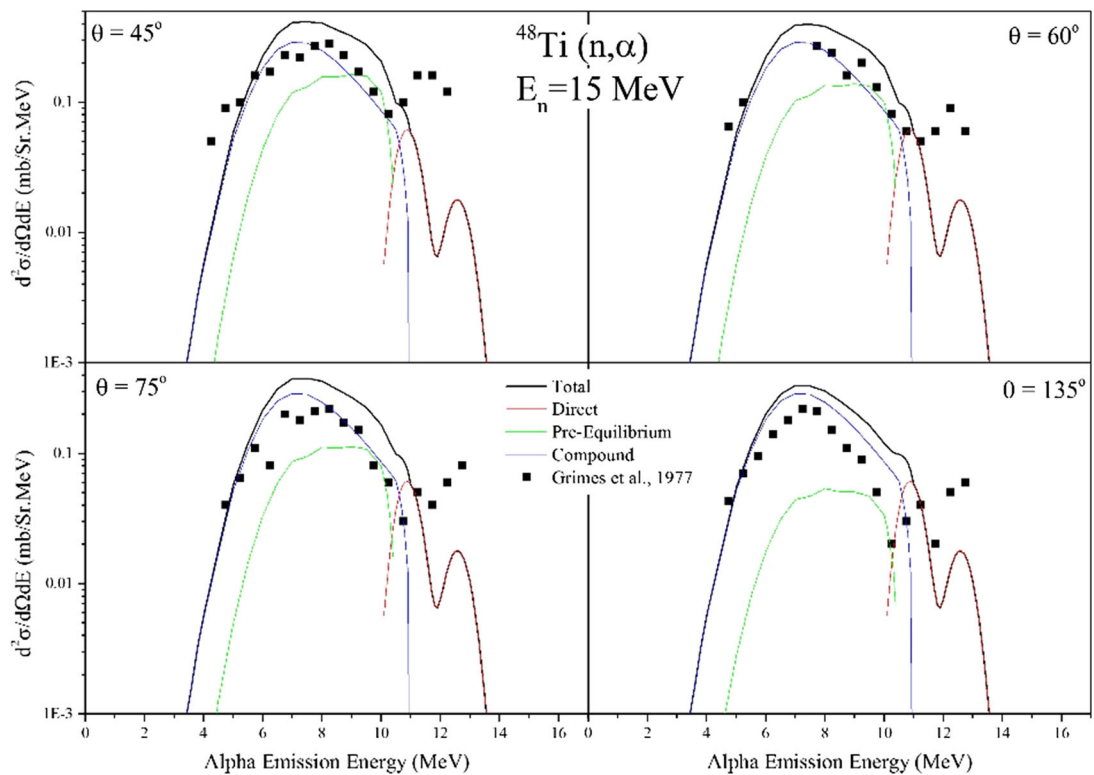

Fig. 2 The comparison of calculated double differential alpha emission cross section for ^{48}Ti target nucleus with the experimental data which are taken from EXFOR [29]
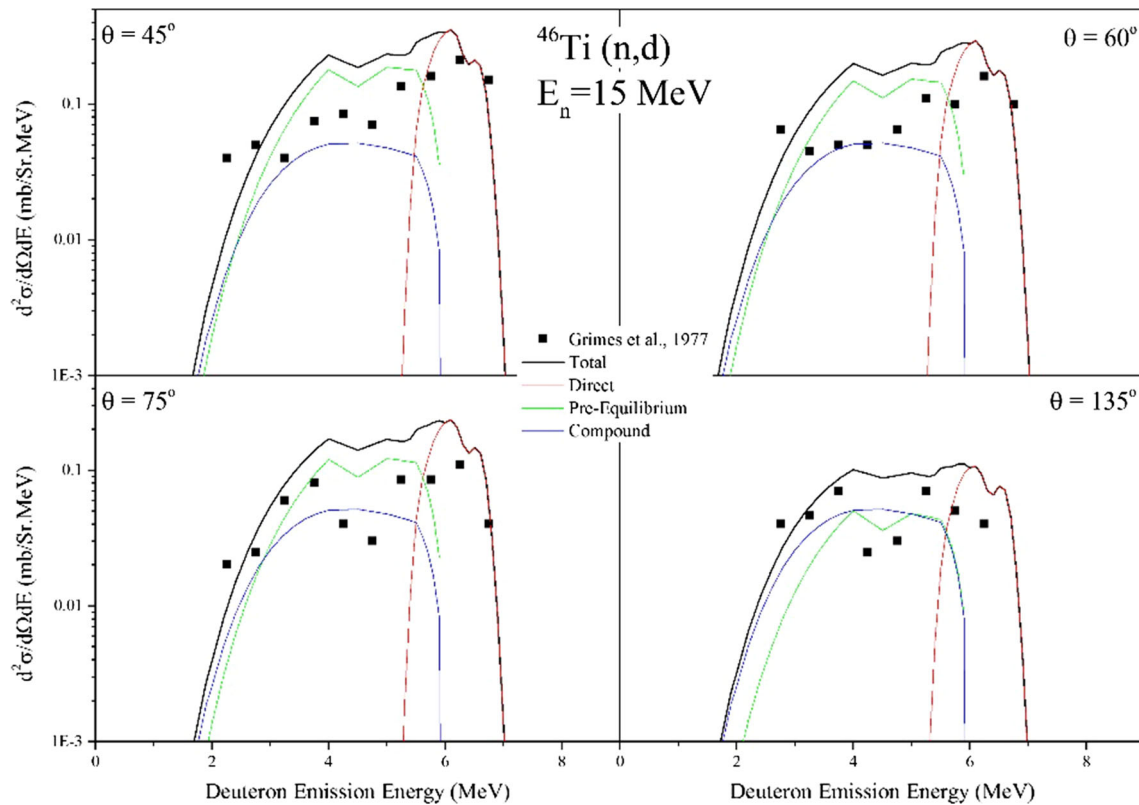
Fig. 3 The comparison of calculated DDX of (n,d) reaction on ^{46}Ti with the experimental data reported in literature. Experimental values were taken from EXFOR [29]

follow the trend with the experimentally measured data by Grimes et al. [28]. Further, the variation in the DDX with the angle of emission of alpha, proton and deuteron particles from ^{46}Ti and ^{48}Ti indicates that the emission of the particles is very close to the isotropic distribution.

Theoretically calculated DDX for the emission of alpha particles from ^{46}Ti(n,α) and ^{48}Ti (n,α) reactions at 15.0 MeV (Figs. 1, 2) show that the alpha particles up to the most probable energies are emitted predominantly through the compound nucleus formation whereas the higher energy alpha particles are emitted through the pre-equilibrium or the direct reaction. While the compound contribution is dominant up to 8 MeV and the pre-equilibrium process is in the range of 8–12 MeV at 45° alpha emission angle, the emission probabilities are very low for energetic alpha particles at 135° emission angle.

The DDX of deuteron emission are compared with experimental data [28] at incident neutron energy 15.0 MeV in Figs. 3 and 4 for ^{46}Ti and ^{48}Ti respectively. The magnitude and shape of calculated results at incident neutron energy 15.0 MeV are in agreement with those of experimental data for deuteron emission all angles. The calculated results of DDX for deuteron emission are mainly from the contribution of the pre-equilibrium emission, and

the contribution of direct emission increases with increasing deuteron emission energy.

The DDX of proton emission are compared with experimental data [28] at incident neutron energy 15.0 MeV as shown in Figs. 5 and 6. The calculated results of DDX for proton emission are mainly from the contribution of the compound emission. While the pre-equilibrium emission contribution is observed after 7 MeV proton emission energy for forward emission angles, it is observed after 9 MeV proton emission energy for 135° backward emission angle. The direct reaction contribution to the proton emission in ^{46}Ti target nucleus is not as much as in ^{48}Ti for the energetic proton emission.

We have completed the description of the light charged particle emission over the full energy range by the compound, direct and pre-equilibrium emission. That calculation scheme has shown that for emission of protons and alphas, almost all charged particles are emitted during the compound stage of the reaction, while for deuteron, a strong component from the pre-equilibrium process is present at low emission energy. In addition, the most important contribution in the equilibrium component originates from the decay of residual nuclei left in an excited state after the pre-equilibrium particle emission.
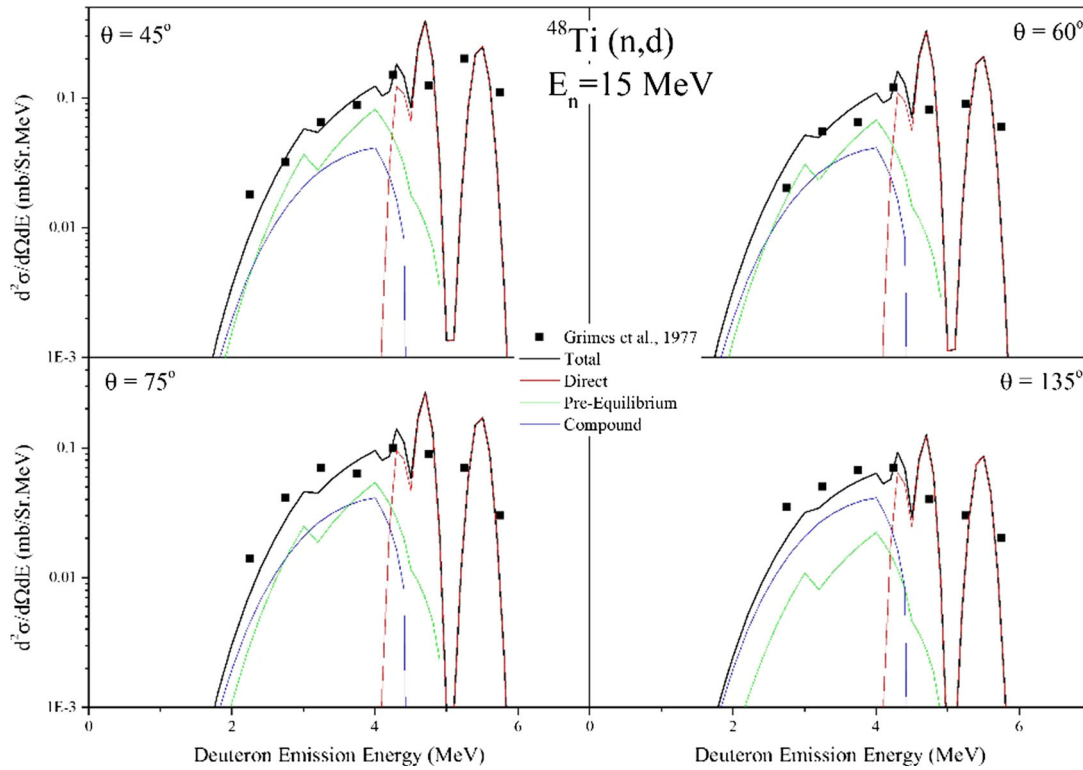
Fig. 4 The comparison of calculated double differential deuteron emission cross section for ^{48}Ti target nucleus with the experimental data which are taken from EXFOR [29]
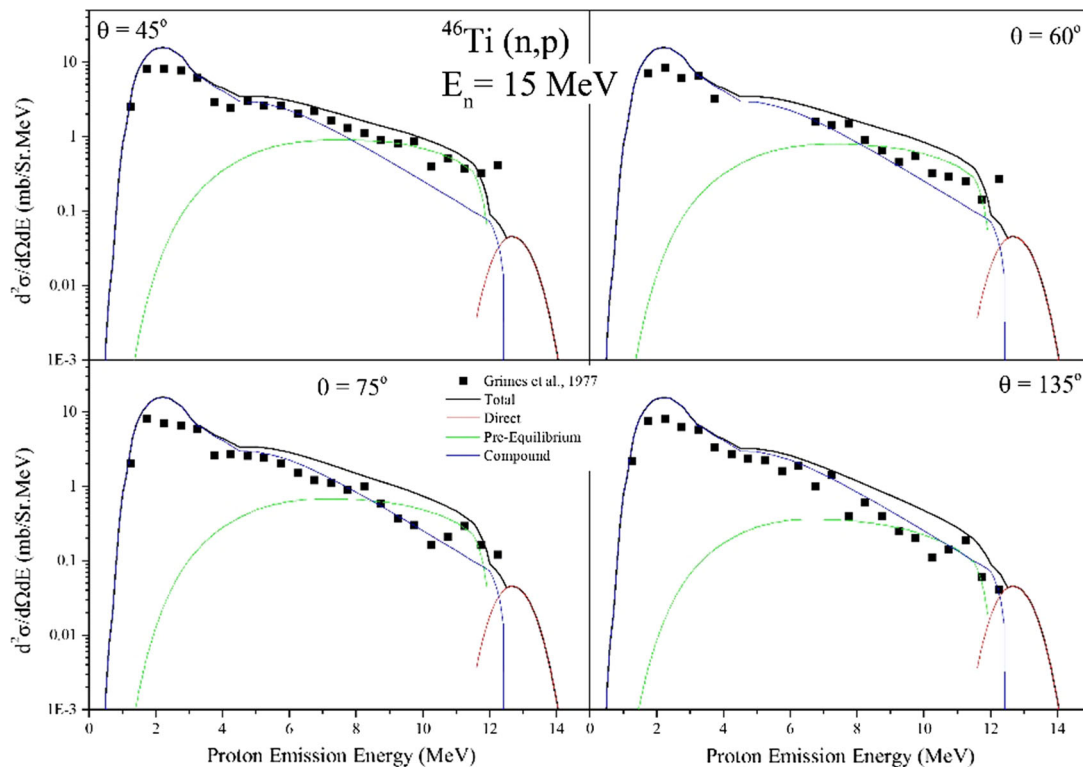

Fig. 5 The comparison of calculated DDX of (n,p) reaction on ^{46}Ti with the experimental data reported in literature. Experimental values were taken from EXFOR [29]
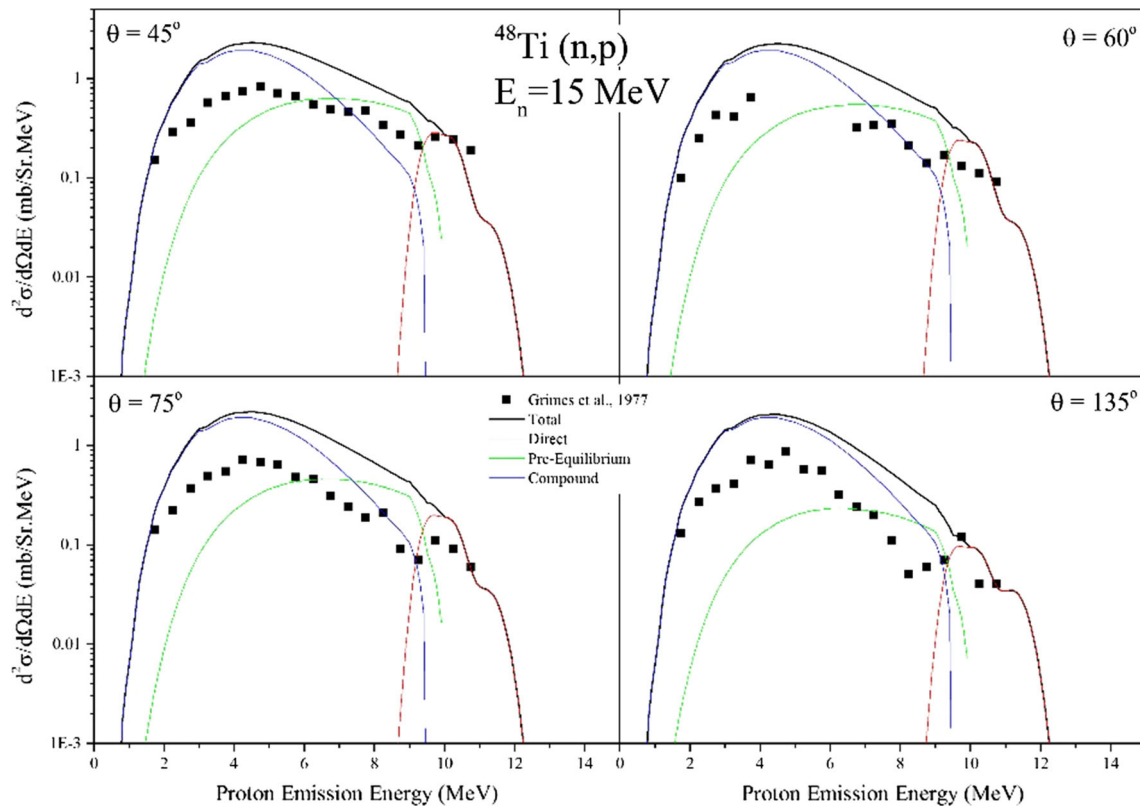
Fig. 6 The comparison of calculated DDX of proton emission for ^{48}Ti target nucleus with the experimental data which are taken from EXFOR [29]

The good reproduction of the shapes of the double differential distributions shows that we obtained with this method suggests that theoretical models must provide at least a good description of the energy-differential cross sections.

References

1. M. Victoria et al., Nucl. Fusion **41**, 1047 (2001)
2. K. Ehrlich, Philos. Trans. R. Soc. SA **357**, 595 (2009)
3. R.A. Forrest, J. Kopercky, "The European Activation System (EASY)" IAEA Advisory Group Meeting on FENDL-2, Vienna (1991)
4. J.W. Davis, D.L. Smith, J. Nucl. Mater. **85–86**, 71 (1979)
5. T. Leguey et al., MRS Symposium on "Microstructural Processes in Irradiated Materials" Fall Meeting, (2000)
6. C.M. Craighead et al., Trans. Metall. Soc. AIME **194**, 1317 (1952)
7. L.W. Berger et al., Trans. Metall. Soc. AIME **212**, 509 (1958)
8. G.A. Lenning et al., Trans. Metall. Soc. AIME **200**, 367 (1954)
9. K. Kondo et al., Fusion Eng. Des. **81**, 1527–1533 (2006)
10. P.M. Prajapati et al., Proceedings of the DAE Symp. on Nucl. Phys. **58**, 456–457 (2013)
11. B. Lalremruata et al., Nucl. Phys. A **821**, 23 (2009)
12. D.W. Kneff et al., Nucl. Sci. Eng. **92**, 491 (1986)
13. Y. Terada et al., J Nucl. Sci. Tech. **39**(2), 413–416 (2002)
14. G.F. Thomas, S.J. Brereton, J Fusion Energ. **4**, 27–44 (1985)
15. A. Kumar et al., J Fusion Energ. **8**, 107–126 (1989)
16. A.A. Cowley et al., Phys. Rev. C **43**, 678 (1991)
17. I.M. Kokooo et al., Nucl. Sci. Eng. **132**, 16–29 (1999)
18. A. Aydin et al., J Fusion Energ. **32**, 378–381 (2013)
19. A. Aydin et al., Phys. Atom. Nucl. **77**(3), 321–324 (2014)
20. Y. Han, Nucl. Phys. A **780**, 34–51 (2006)
21. J.-F. Duan et al., Commun. Theor. Phys. **54**, 129–137 (2010)
22. I.H. Sarpün et al., J. Nucl. Sci. **1**(1), 1–5 (2014)
23. Z. Zhang et al., Ann. Nucl. Energ. **37**, 130–143 (2010)
24. A.J. Koning, J.P. Delaroche, Nucl. Phys. A **713**, 231 (2003)
25. A.J. Koning, et al. TALYS-1.6, User manual. http://www.talys.eu/
26. A.J. Koning, M.C. Duijvestijn, Nucl. Phys. A **744**, 1576 (2004)
27. K. Kalbach, Phys. Rev. C **71**, 034606 (2005)
28. S.M. Grimes et al., Nucl. Sci. Eng. **62**, 187 (1977)
29. EXFOR/CSISRS, National Nuclear Data Center. http://www.nndc.bnl.gov/exfor/exfor00.htm